Analytical Methods

Accepted Manuscript

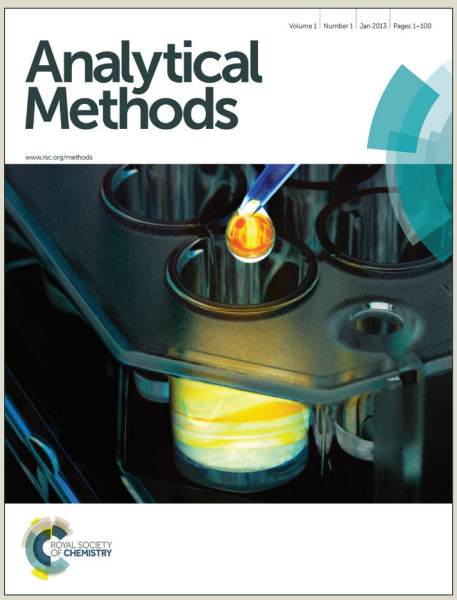

ROYAL SOCIETY OF CHEMISTRY

www.rsc.org/methods

Journal Name

RSCPublishing

ARTICLE

Microwave-assisted aqueous synthesis of Mn-doped ZnS quantum dots and their room-temperature phosphorescence detection of indapamide

Cite this: DOI: 10.1039/xoxxoooooox

Received ooth January 2012,
Accepted ooth January 2012

DOI: 10.1039/xoxxoooooox

www.rsc.org/

Dong Zhu,* Wei Li,* Hong-Mei Wen, Qian Chen, Li Ma and Yue Hu

Mn-doped ZnS quantum dots (QDs) prepared by conventional aqueous synthetic method usually suffer from poor crystallinity and low quantum yield due to relatively low reaction temperature. In this paper, high-quality Mn-doped ZnS QDs with long-lived emission were prepared using a green and rapid microwave-assisted synthetic approach in aqueous solution. The QDs were used for the room-temperature phosphorescence (RTP) detection of indapamide with the detection limit of 0.89 μM, and RTP intensity showed a good linear relationship with the concentration of indapamide in the range of 1.5 to 80 μM. The relative standard deviation for seven independent measurements of 10 μM indapamide was 3.4%, and the recovery ranged from 94% to 105%.

Introduction

Mn-doped ZnS quantum dots (Mn-ZnS QDs) have attracted considerable attention in the past decade, due to their strong and stable emission from the $^4T_1 \rightarrow {}^6A_1$ transition of Mn^{2+} in the ZnS host lattice.[1-4] The low toxicity and high photoluminescence quantum yield (QY) of Mn-ZnS QDs, plus the excellent stability, make the QDs a promising optical label for biological imaging and biosensor.[5-8] Additionally, the large Stokes shift of the emission effectively reduces its self-quenching, enabling the Mn-ZnS QDs to be used in optoelectronics, such as LEDs and solar cells.[9-10] More importantly, when combined with the technique of time-resolved luminescence that utilizes the long-lived emission of Mn^{2+} by setting appropriate delay time, the short-lived background luminescence or interferences such as scattered lights and auto fluorescence can be effectively suppressed, which thus enable the Mn-ZnS QDs as excellent room temperature phosphorescence (RTP) probes.[11-18]

In the past decade, various approaches were reported to synthesize the Mn-ZnS QDs, mostly focused on high-temperature organometallic routes[19-23] and aqueous synthesis.[24-27] The Mn-ZnS QDs prepared by the high-temperature organometallic method had high quantum yield, high crystallinity and monodispersity. However, unavoidable hazardous organic reagents in the synthesis, long reaction time and limited operation conditions confined their applications. The direct aqueous synthetic method has been proved to be simpler, cheaper and less toxic to prepare the water-soluble Mn-ZnS QDs. However, the Mn-ZnS QDs synthesized by this method usually suffer from poor crystallinity and low QY due to low reaction temperature (which is only less than 100℃) and long reaction time. Furthermore, some defects of photoluminescence still existed in the prepared Mn-ZnS QDs such as the dual emissions from the band edge emission and dopant emission, [30, 31] which would limit their applications in certain fields.[32] Therefore, development of a safe and environment-friendly synthesis of the Mn-ZnS QDs with pure dopant emission, stronger luminescence and better photostability is critical for the further application. Recently, a microwave-assisted hydrothermal procedure was used for the synthesis of diverse nanomaterials.[33-35] It exhibited many distinct advantages over conventional synthesis in aqueous solution such as relatively high reaction temperature (up to 200 ℃), rapid heating to crystallization temperature, fast supersaturating by the rapid dissolution of precipitated gels, and eventually a shorter crystallization time compared with conventional external heating.[34]

Herein, we report a green and rapid synthesis of the Mn-ZnS QDs in aqueous solution by microwave irradiation. The prepared Mn-ZnS QDs not only hold high crystallinity and monodispersity, but also exhibit excellent water-solubility and high photoluminescence. A room-temperature phosphorescence

College of Pharmacy, Nanjing University of Chinese Medicine, Nanjing 210023, P. R.China.
*E-mail: dongzhunjutcm@hotmail.com; liwaii@126.com;
Fax: +86 2585811839; Tel: +86 25 85811839

† Electronic supplementary information (ESI) available: XRD, FT-IR, RTP spectral of and fluorescence spectra of Mn-ZnS QDs.

was demonstrated to determine indapamide in practical samples using the Mn-ZnS QDs as the phosphorescence probe. Indapamide belongs to the class of thiazide-type diuretic drugs and is widely used in the treatment of hypertension , nephrogenic diabetes insipidus and nephrolithiasis.[36-37] The determination of indapamide is very important taking into account that its overdose might lead to severe hyponatraemia, with symptoms varying from nausea to seizures and coma and hypokalemia,[40,42] which could lead to fatal arrhythmia.[43] Compared with the traditional high performance liquid chromatography (HPLC) detection methods, [44-48] the Mn-ZnS QDs-based RTP method was facile and rapid for the detection of indapamide because the troublesome sample pretreatment and gradient elution could be avoided.

Experimental Section

Chemicals.

Indapamide, as a standard sample, was purchased from the National Institute for the Control of Pharmaceutical and Biological Products. 3-Mercaptopropionic acid (MPA) was from Fluka. $Zn(NO_3)_2$, Na_2S, $MnCl_2$ and sodium palmitate were obtained from Shanghai Reagent Company. Ethanol (CH_3CH_2OH, anhydrous) was of analytical grade and used without further purification. Other chemicals were of analytical grade. Phosphate buffer solution (PBS, 25 mM, pH = 7.4) was prepared by mixing the solutions of K_2HPO_4 and NaH_2PO_4. All of these reagents were of analytical reagent grade and used as received without further purification. Puried water from a Milli-Q-RO4 water purification system (Millipore, Simplicity, MA, USA) with a resistivity higher than 18 $M\Omega \cdot cm^{-1}$ was used to prepare all solutions.

Apparatus and Characterization.

A microwave synthesis system (CEM Discover) made by CEM Instruments (USA) was used for the preparation, which was equipped with controllable temperature and pressure units. The system can operate at 2450 MHz frequency and work at 0-300 W power. The reaction temperature, pressure and time can be programmed by users. The synthesis of Mn-ZnS QDs was preformed in a cylindrical digestion vessel that was high-strength vessel consisting of a special kind of glass. The volume of vessel used in the reaction was 80 mL. X-ray diffraction (XRD) measurements were performed on a Shimadzu XRD-6000 powder X-ray diffractometer, using Cu Kα (λ = 1.5405 Å) as the incident radiation. Transmission electron microscopy (TEM) and high-resolution TEM (HRTEM) samples were prepared by dropping the samples dispersed in water onto carbon-coated copper grids with excess solvent evaporated. TEM images were recorded on a Shimadzu JEM-2010 CX with an accelerating voltage of 100 kV. HRTEM images were recorded on a JEM-2010 F with an accelerating voltage of 200 kV. UV-vis absorption spectra were obtained using a UV-3600 spectrophotometer (Shimadzu). Inductively coupled plasma atomic emission spectroscopy (ICP-AES) was performed on a Perkin-Elmer Optima 3000 DV after dissolving the aqueous Mn-ZnS QDs in 5% hydrochloric acid. Fluorescence measurements were performed using a Shimadzu RF-5301 PC fluorescence spectrometer. The room-temperature photoluminescence quantum yield of the Mn-ZnS QDs was estimated following the ref 38-39 by using quinine sulfate as a reference standard. The phosphorescence lifetime of the Mn-ZnS QDs was measured with a FLS 920 spectroscope (Edinberge). The phosphorescence spectrum was performed on an LS-55 fluorometer (Perkin-Elmer). All of the measurements were performed at room temperature.

Microwave-assisted aqueous synthesis of the Mn-ZnS QDs

Scheme 1 illustrated the microwave-assisted aqueous synthesis of Mn-ZnS quantum dots. In a typical experiment, 2.0 g sodium palmitate was added to the mixture of 15 mL water and 5 mL ethanol, and the pellucid solution was obtained. Then 10 mL of aqueous solution containing 0.25 g of zinc nitrate and 0.02 g of manganese chloride, and 5 mL freshly Na_2S solution was added sequently to the sodium palmitate solution. The typical molar ratio of Zn^{2+}:S^{2-} was 2:1 in our experiments. The mixture was transferred to an 80 mL cylindrical digestion vessel under agitation. The reaction was maintained at 170 °C and 180 psi for 35 min under microwave irradiation (260W). The Mn-ZnS QDs that collected at the bottom of the container were redispersed in 50 mL of chloroform. After centrifugation at 6 000 rpm, the transparent upper Mn-ZnS QDs solution was collected. The solution was dried in vacuum, and the Mn-ZnS QDs powders of about 80 mg were obtained.

The Mn-ZnS QDs coated with the original alkyl ligands were dissolved in 20 mL of chloroform and treated with 200 μL of MPA. The mixture was shaken for 60 min under sonication. The chloroform solution gradually became turbid because the original ligands with a long hydrophobic alkyl chain were replaced by the hydrophilic carboxyl chain of MPA. The MPA-coated Mn-ZnS QDs precipitate was isolated by centrifugation and decantation. Excess MPA was further removed by washing the precipitate with chloroform for three times. The final precipitate was dried in vacuum, and then the Mn-ZnS QDs powders were obtained. The powders can be dispersed to PBS solution (pH 7.4). The content of the incorporated Mn^{2+} in the Mn-ZnS QDs was determined by ICP-AES after dissolving the Mn-ZnS QDs in 5% hydrochloric acid solution.

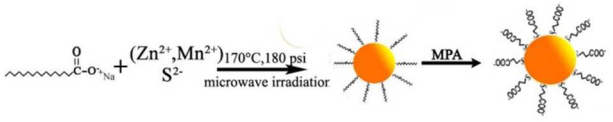

Scheme 1. Schematic representation of microwave-assisted aqueous synthesis of Mn-doped ZnS quantum dots.

Indapamide standard samples were dissolved in 0.1M NaCl solution. Human urine samples were collected from healthy people and centrifuged at 3500 rpm for 10 min to remove particulates. The samples were subjected to a 50-fold dilution before analysis. All experiments were performed in compliance

with the relevant laws and institutional guidelines. And the test objects were told and consented.

Room-temperature phosphorescence detection of indapamide.

To a 10 mL calibrated test tube, 4.0 mL of 10 mg·L^{-1} MPA-capped Mn-ZnS QDs solution, 5.0 mL of PBS (0.1 M, pH 8.0) and different volumes of indapamide standard solution were added in order. The mixture was then diluted to 10 mL with double distilled water and mixed completely. After reacting for 5 min, the phosphorescence intensity of the solution was measured at an excitation wavelength of 310 nm, delay time of 0.2 ms, gate time of 0.4 ms, and cycle time of 20 ms in the absence or presence of a series of indapamide solutions.

Results and discussion

Characterization of the Mn-ZnS QDs

The morphology of the Mn-ZnS QDs was characterized with high resolution transmission electron microscopy (HRTEM). As demonstrated in Figure 1, the QDs showed high crystallinity and monodispersity. The average size of the Mn-ZnS QDs was about 4.2 nm. The HRTEM image of one individual Mn-ZnS quantum dot indicated the distances between the adjacent lattice fringes to be 0.33 nm, corresponding with the literature value for the (111) d spacing, 0.324 nm (JCPDF No. 77-2100). The good crystallinity and high quality of the Mn-ZnS QDs can be attributed to the uniform and fast heating under microwave irradiation.

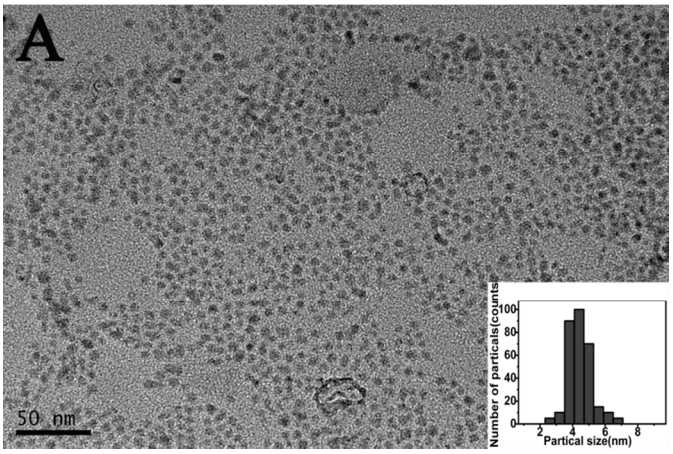

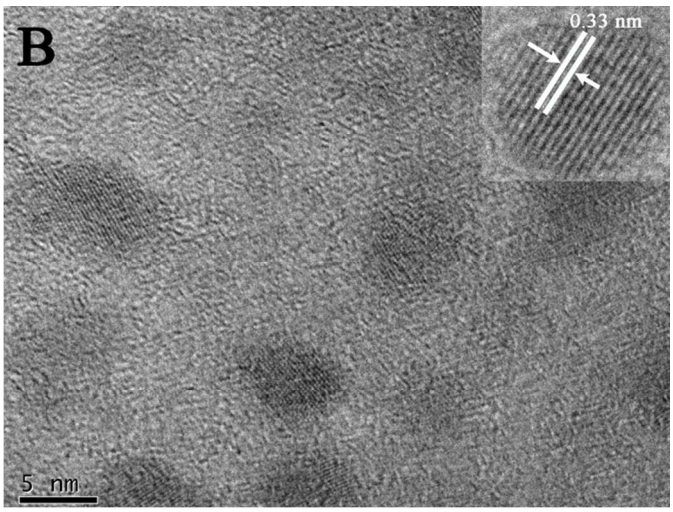

Figure 1. (A) TEM image of the Mn-ZnS QDs. Bottom inset: the size distribution histogram. The size distribution histogram was obtained by averaging the sizes of 200 particles from the TEM image. (B) HRTEM image of the Mn-ZnS QDs. Top inset: HRTEM image of one individual nanocrystal

The crystallinity of the Mn-ZnS QDs was demonstrated by powder X-ray diffraction (XRD) as shown in Figure 2. The intense and wide peaks, characteristic for nanoparticles, are positioned at 2θ= 28.7°, 48.1°, and 56.4°, which oriented along the (111), (220), and (311) directions, and are in agreement with the card JCPDS No.77-2100 for cubic zinc blende ZnS. Compared with the Mn-ZnS QDs prepared by the traditional aqueous method with reference 20 as shown in Figure S1 (See Supplement Information), the XRD peak of our microwave-assisted aqueous synthetic sample have stronger intense especially for (220), and (311) directions, which showed the crystallininty enhancement. The incorporated Mn concentration in the Mn-ZnS QDs was determined by inductively coupled plasma atomic emission spectroscopy (ICP-AES).

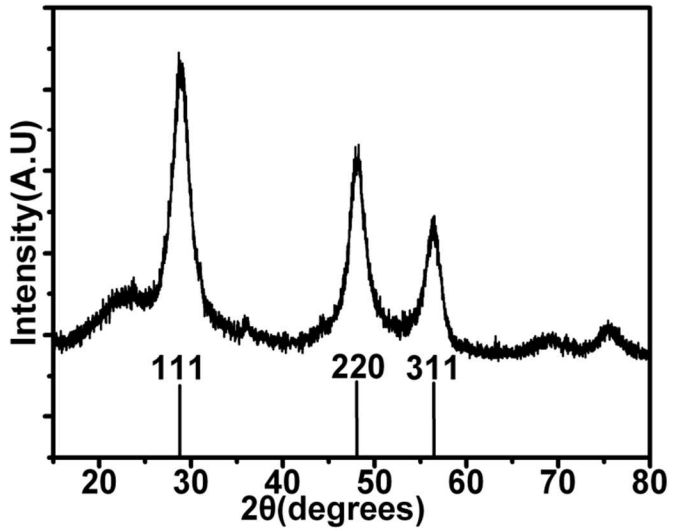

Figure 2. XRD patterns of the Mn-ZnS QDs. Diffraction lines for cubic phases of bulk ZnS are shown for the guidance

Figure 3 shows the typical UV-vis absorption spectra and photoluminescence (PL) spectra of the Mn-ZnS QDS. As shown in Figure 3, a small peak at 314 nm was attributed to the formation of an exciton of the intrinsic ZnS nanocrystals. The inset was corresponding fluorescence and RTP spectra of the QDs. The fluorescence spectra display two photoluminescence emission peaks when excited at 310 nm. The weak blue emission around 420 nm is attributed to the defect-related emission of the ZnS, and the other strong orange emission with a symmetric peak around 585 nm can be attributed to the $_4T^1 \rightarrow {}_6A^1$ transition of the Mn^{2+} in the ZnS host lattice.[1-4] While in the RTP spectra, the emission around 420 nm was completely avoided due to the short lifetime of the ZnS defect-related emission. The photoluminescence effect of various Mn:Zn ratio was also studied in prepared QDs as shown in ESI. The PL quantum yield (QY) of the Mn-ZnS QDs was up to 18%.

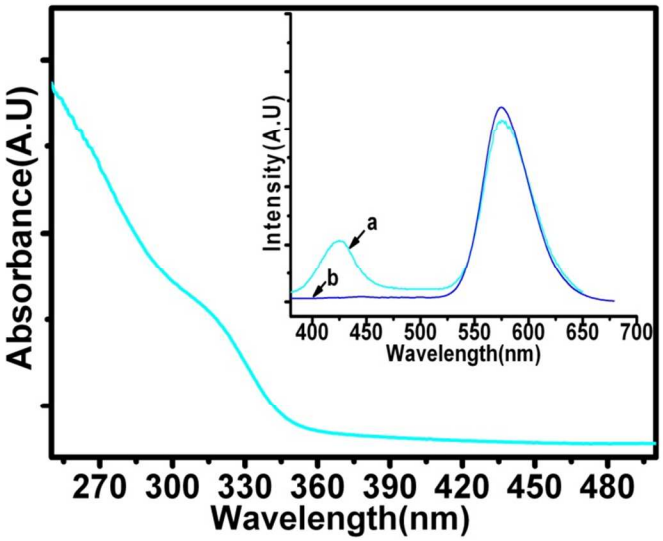

Figure 3. UV absorption spectra of the Mn-ZnS QDs in water. The inset was corresponding fluorescence (a) and RTP (b) spectra of the QDs.

The phosphorescence life-time of 1.2 ms for the strong orange emission attributed to the $_4T^1 \rightarrow {}_6A^1$ transition was also evaluated from the decay curve of the phosphorescence emission of Mn-doped ZnS QDs as shown in Figure 4.

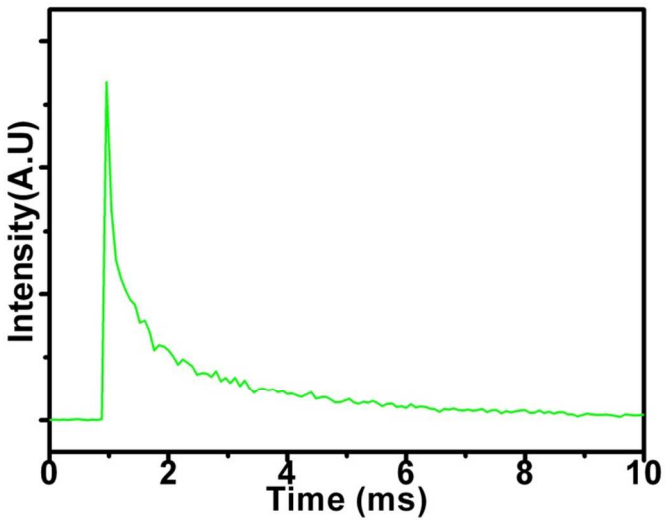

Figure 4. The decay curve of the phosphorescence emission of Mn- ZnS QDs

RTP detection of indapamide

RTP detection of indapamide was established by using the Mn-ZnS QDs as a probe. The carboxylic groups on the surface of the MPA-capped Mn-ZnS QDs acted as the receptor sites to bind the -NH groups of indapamide species. The binding of indapamide onto the surface of the Mn-ZnS QDs was confirmed using infrared spectroscopy as shown in Supporting Information Figure S3, which can effectively quench the phosphorescence intensity of the Mn-ZnS QDs.

The quenched RTP intensity and initial RTP intensity without adding indapamide from pH 4.0 to 10.0 are indicated in Figure 5. The quenched phosphorescence intensity increased slowly as the pH value varied from 4 to 7, and then increased rapidly from pH 7 to 8 as shown in Figure 5 (A). Further increase in pH value from 8 to 10 decreased the quenched phosphorescence intensity. It is also possible that the pH effect is associated with the interaction of indapamide with the Mn-ZnS QDs. The amino group of indapamide is deprotonated at pH > 8.8 (pKa), which benefits the adsorption between indapamide and carboxyl group on the surface of the QDs.[41] Thus, the quenched phosphorescence intensity achieved maximum at pH 8 in our pH conditional experiment. Additionally, the phosphorescence intensity of the Mn-ZnS QDs is also pH-dependent. With the increase of pH, the deprotonation of the thiol group of the MPA capping molecules enhanced the covalent bond between the QDs and the capping molecules, resulting in an increase of phosphorescence intensity. But too high pH (pH> 8) value could cause the decrease of quenched RTP intensity, thus bring the decrease of sensitivity. Considering the two factors, the optimal condition was chosen as pH 8.0 for the detection of indapamide in the following studies.

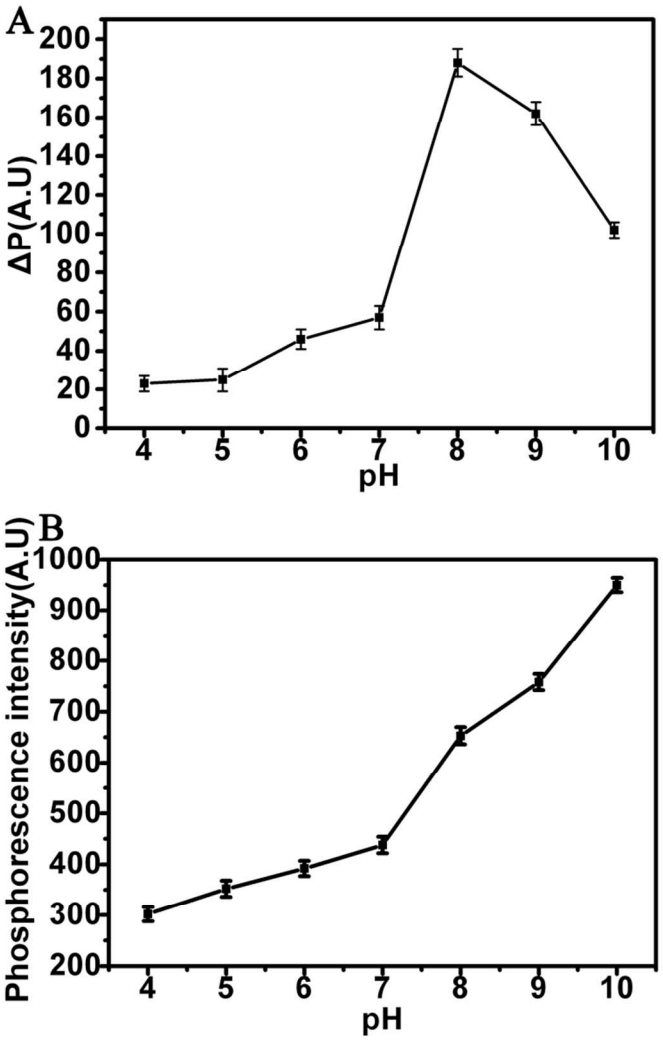

Figure 5. (A). Effect of pH on the quenched phosphorescence of the Mn-ZnS QDs (10 mg·L^{-1}) by indapamide (5 μM). (B). Effect of pH on the phosphorescence of the Mn-ZnS QDs in the absence of indapamide.

Figure 6 displays the effect of reaction time on the phosphorescence intensity of 10 mg·L^{-1} Mn-ZnS QDs with 30 μM indapamide in PBS (pH 8.00). The RTP intensity of the Mn-ZnS QDs was quenched quickly upon addition of indapamide firstly, and the reaction reached equilibrium within 5 min. Furthermore, the RTP intensity of this system remained stable over half of an hour. Therefore, the detection of samples was appropriated after 5 min reaction.

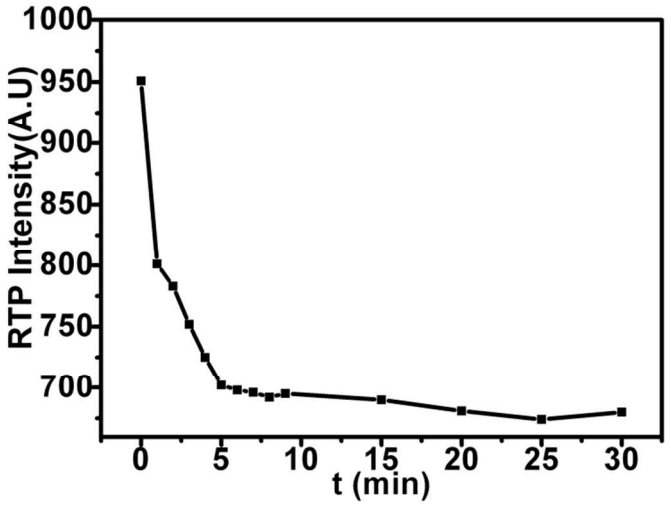

Figure 6 Effect of time on the RTP intensity of 10 mg•L^{-1} Mn-ZnS QDs upon addition of 30 μM indapamide (λ_{ex}: 310 nm, with pH 8.0 PBS solution).

As shown in Figure 7 (A), the quenching of the RTP intensity of the Mn-ZnS QDs was dependent on the concentration of indapamide. The phosphorescence quenching followed the Stern-Volmer's equation:

$$P_0/P = 1 + Kc$$

where P_0 and P are the phosphorescence intensities in the absence and presence of indapamide, respectively, c is the concentration of the analyte and K is the quenching constant of the quencher. This quenching equation was consistent with previous reports.[13,14] Figure 7 (B) shows a linear calibration plot of the quenched PL intensity against the concentration of indapamide in the range of 1.5-80 μM with a correlation coefficient of 0.995. The relative standard deviation for eleven repeated measurements of 10 μM indapamide was 3.4% (RSD), and the detection limit was 0.89 μM which was calculated by 3 δ /k (where δ is the standard deviation for 11 replicate determinations of the blank solution and k is the slope of the standard curve).

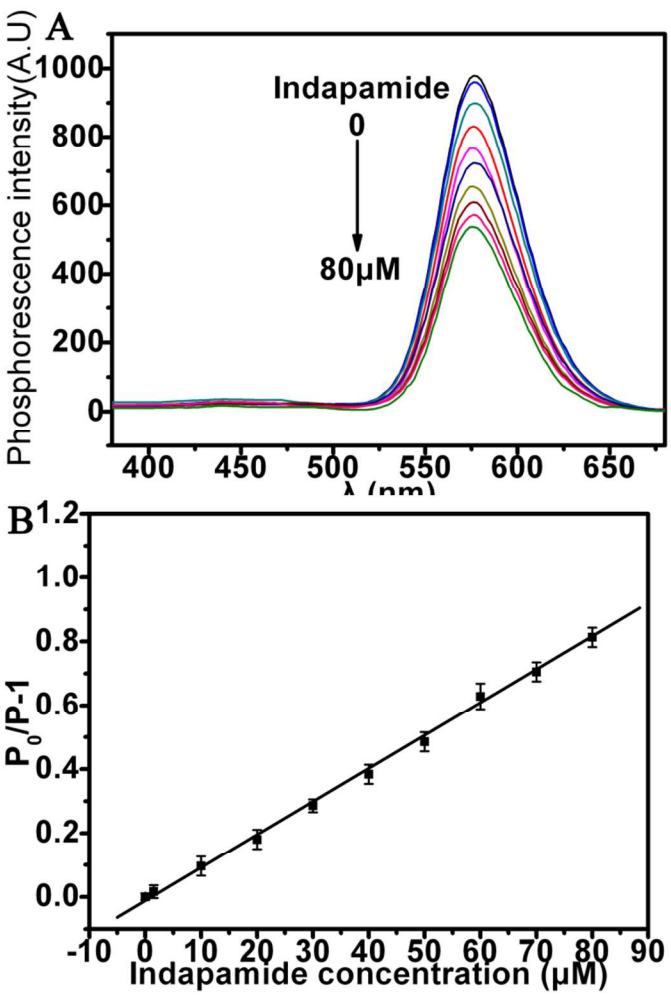

Figure 7 (A) Phosphorescence spectra of the Mn-ZnS QDs with different indapamide concentrations. (B) Calibration curve for indapamide. The concentrations of indapamide (0-80, μM) are 0, 1.5, 10, 20, 30, 40, 50, 60, 70, 80. RTP measurement condition: excitation wavelength, 310 nm; delay time, 0.2 ms; gate time, 0.4 ms; cycle time, 20 ms. Error bars mean the standard deviation. Each point was an average value of three independent measurements.

Interference of coexisting chemicals

The Mn-ZnS QDs gave excellent selectivity for RTP detecting indapamide in the presence of main relevant metal ions in biological fluids, glucose, and some small biomolecules such as amino acids. The influence of these components on the Mn-ZnS QDs with 30 μM indapamide was shown in Table 1. The results indicated that none of these coexisting substances produced a detectable effect, showing deviations of the RTP signal of less than 10%.

Table 1 Effect of co-existing substances on the quenched RTP intensity of the Mn-ZnS QDs

Co-existing substances	Concentration (μM)	ΔI_P (%)
Glucose	1000	-2.5
L-cysteine	1200	+3.1
Histidine	1200	+2.9
Aspartic acid	1200	-1.8
Serine	1200	-3.5
Methionine	1200	-4.2
Leucine	1200	3.6
Na^+	5000	1.9
K^+	5000	1.4
Ca^{2+}	5000	2.3
Mg^{2+}	5000	1.4
Zn^{2+}	5000	2.0

Application of the Mn-ZnS QDs-based RTP method to the dectection of practical samples.

Figure S4 compares the fluorescence and RTP spectra of the Mn-ZnS QDs in human serum and urine. No RTP background from urine and serum was observed in the phosphorescence mode, although the fluorescence background from urine (Figure S1, curve b) and serum (Figure S4, curve a) was significant. Under optimal conditions, the Mn-ZnS QDs-based RTP method was used to detect indapamide in urine. As seen in Table 2, the results of this proposed method were in good agreement with the results obtained by liquid chromatography.[46] The recovery of spiked indapamide was 94-105%. These results indicated that the Mn-ZnS QDs was successful in RTP detection of indapamide in urine sample.

Table 2. Recovery (mean± SD; n = 3) for determination of indapamide in urine by using the phosphorescence of QDs and the reference method [46]

Sample	Spiked concn(μM)	Proposed method Result (μM)	recovery (%)	Reference method Result (μM)	recovery (%)
Urine	0	Not detected	–	Not detected	–
Urine	15	14.1±0.6	94±4	14.5±0.3	97±2
Urine	30	31.5±1.2	105±4	30.5±0.3	102±1
Urine	45	46.4±1.8	103±4	45.6±0.3	101±1

Table 3 compares the figures of merit of the proposed method with other reported methods for the determination of indapamide. It can be clearly seen from the table that the total analytical time used in the proposed method is highly minimal, and the limits of detection (LOD) are not enough lowly, but enable to deal with routine detection compared with other methods. These advantages and disadvantages emphasize the fact that the proposed method is facile, rapid and highly cost

Table 3 Comparison of the proposed method with other methods

Method	LOD (μM)	Total analytical time (min) [a]	Reference
HPLC-ESI-MS[b]	0.002	30	47
HPLC-UV[c]	0.01	30	46
HPLC–UV[c]	0.05	25	48
RTP	0.89	5	Present method

[a] Total analytical time refers to the overall time taken for the analytical procedure, including ultrasonication, centrifugation ,vortex mixing and elution time wherever applicable. [b]ESI-MS – Electrospray ionization-mass spectrometry. [c] UV-UV-Vis detection.

effective, which could meet the requirements of prompt determination for indapamide because the troublesome sample pretreatment and gradient elution could be avoided.

Conclusions

In conclusion, high-quality Mn-ZnS QDs were successfully synthesized by a green and rapid microwave-assisted aqueous synthetic approach. The obtained Mn-ZnS QDs not only have high crystallinity and monodispersity, but also exhibit excellent water-solubility and high photoluminescence. A RTP method was established to determine indapamide in urine using the Mn-ZnS QDs as RTP probe, which supported that the Mn-ZnS QDs were a promising material for RTP detection.

Acknowledgements

We greatly appreciate the National Natural Science Foundation of China for the financial support (21205064). This work was also supported by Fund of State Key Laboratory of Analytical Chemistry for Life Science (SKLACLS1208). We also greatly appreciate "A Project Funded by the Priority Academic Program Development of Jiangsu Higher Education Institutions".

Notes and references

1 D. J. Norris, A. L. Efros and S. C. Erwin, *Science*, 2008, **319**, 1776.
2 X.Michalet, F. F. Pinaud, L. A. Bentolila, J. M. Tsay, S. Doose, J. J. Li, G. Sundarensan, A. M. Wu, S. S. Gambhir and S. Weiss, *Science*, 2005, **307**, 538;
3 R. G. Xie, D. Battaglia and X. G. Peng, *J. Am. Chem. Soc*., 2007, **129**, 15432;
4 R. G. Xie and X. G. Peng, *Angew. Chem., Int. Ed*., 2008, **47**, 7677.
5 D. Mocatta, G. Cohen, J. Schattner, O. Millo, E. Rabani and U. Banin, *Science*, 2011, **332**, 77-81.
6 K. Manzoor1, S.Johny, D.Thomas, S.Setua, D. Menon and S. Nair *Nanotechnology* , 2009, **20**, 065102
7 W. S. Zou, D. Sheng, X. Ge, J. Q. Qiao and H. Z. Lian, *Anal. Chem*., 2011, **83**, 30.
8 R.Ban, J-J. Li, J.T.Cao, P.H. Zhang, J.R. Zhang and J-J. Zhu, *Anal. Methods*, 2013,**5**, 5929-5937.
9 P. T. Shao, H. Z. Wang, Q. H. Zhang and Y. Li, *J. Mater. Chem*., 2011, **21**, 17972.
10 P. K. Santra and P. V. Kamat, *J. Am. Chem. Soc*., 2012, **134**, 2508-2511.
11 P. Wu and X.-P. Yan, *Chem. Soc. Rev*., 2013, **42**, 5489-5521.
12 H.-F. Wang, Y. Li, Y.-Y. Wu, Y. He and X.-P. Yan, *Chem. - Eur.J.*, 2010, **16**, 12988.
13 Y. He, H.-F. Wang and X.-P. Yan, *Anal. Chem*., 2008, **80**, 3832.
14 H.-F. Wang, Y. He, T.-R. Ji and X.-P. Yan, *Anal. Chem*., 2009, **81**, 1615.
15 P. Wu, Y. He, H.-F. Wang and X.-P. Yan, *Anal. Chem.*, 2010, **82**, 1427.
16 P. Wu, L.-N. Miao, H.-F. Wang, X.-G. Shao and X.-P. Yan, *Angew. Chem., Int. Ed*., 2011, **50**, 8118.
17 W. S. Zou, D. Sheng, X. Ge, J. Q. Qiao and H. Z. Lian, *Anal. Chem*., 2011, **83**, 30.
18 D. Zhu, W. Li, L. Ma and Y. Lei, *RSC Adv*., 2014, **4**, 9372
19 V. M. Frederic, K. Masaru, B. Marina, A.H. Dennis, G. G. Robert and G.B. Moungi, *J. Am. Chem. Soc*. 2000, **122**, 2532
20 J. Zheng, X. Yuan, M. Ikezawa, P. Jing, X. Liu, Z. Zheng, X. Kong, J. Zhao and Y. Masumoto, *J. Phys. Chem. C*, 2009, **113**, 16969.
21 W. Zhang, Y. Li, H. Zhang, X. Zhou and X. Zhong, *Inorg. Chem*.,2011, **50**, 10432.
22 B. B. Srivastava, S. Jana, N. S. Karan, S. Paria, N. R. Jana, D. D. Sarma and N. Pradhan, *J. Phys. Chem. Lett*., 2010, **1**, 1454.
23 J. Zheng, W. Ji, X. Wang, M. Ikezawa, P. Jing, X. Liu, H. Li, J. Zhao and Y. Masumoto, *J. Phys. Chem. C*, 2010, **114**, 15331.
24 J. Zhuang, X. Zhang, G. Wang, D. Li, W. Yang and T. Li, *J. Mater. Chem*., 2003, **13**, 1853-1857.
25. W. Jian, J. Zhuang, W. Yang and Y. Bai, *J. Lumin*., 2007, **126**, 735-740.
26. Q. Xiao and C. Xiao, *Opt. Mater.*, 2008, **31**, 455.
27 A. Abdelhay, G. Malgorzata, B. Lavinia, G. Jaafar, M. Ghouti, and S. Raphaël, *Inorg. Chem*., 2010, **49 (23)**, 10940.
28. S.-Q. Chang, B. Kang, Y.-D. Dai, H.-X. Zhang and D. Chen, *Nanoscale Res. Lett*., 2011, **6**, 591.
29. R. Begum, S. Bhandari and A. Chattopadhyay, *Langmuir*, 2012, **28**, 9722-9728.
30 D. J. Norris, N. Yao, F. T. Charnock and T. A. Kennedy, *Nano Lett*., 2001, 1, 3-7.
31 L. J. Zu, A. W. Wills, T. A. Kennedy, E. R. Glaser and D. J. Norris, *J. Phys. Chem. C*, 2010, **114**, 21969-21975.
32 D. Mocatta, G. Cohen, J. Schattner, O. Millo, E. Rabani and U. Banin, *Science*, 2011, **332**, 77-81.
33 M. A. Correa-Duarte, M.Giersig, N. A. Kotov and L. M. Liz-Marzan, *Langmuir* ,1998, **14**, 6430–6435.
34 L.Li, H. F. Qian and J. C. Ren, *Chem. Commun*. 2005, 528–530.
35 L. N. Bharat, O. Johnson and K. Sridhar, *J. Phys. Chem. B* 2001,**105**, 8356–8360.
36 F. A. Krumlovsky and F. del Greco, *Postgrad. Med.*, 1976, 59, 105–110.
37 J. G. Hardman and L. E. Limbird, Goodman and Gilman's *Pharmacological Basis of Therapeutics*, McGraw-Hill, New York, 9th edn, 1996.
38 IUPAC, Reference materials for fluorescence measurement, *Pure Appl. Chem.*, 1988, **60(7)**, 1107–1114.
39 J. N. Demas and G. A. Crosby, *J. Phys. Chem*., 1971, **75**, 991.
40 D. A. Sica, *J. Clin. Hypertens*., 2004, **6**, 532–540
41 D.L.Dong, Q.H.Wang, P.Yue, J.D.Jiao, R.M.Gu and B.F.Yang *Eur.J Pharmacol*. 2006, **24**, 536(1-2), 78-84.
42 M. D. Chapman, R. Hanrahan, J. McEwen and J. E. Marley, *Med. J. Aust*., 2002, **176**, 219–221.
43 N. Ohashi, S. Minemura, A. Togawa and K. Ohyama, *Clin. Exp. Nephrol*., 2011, **15**, 761–764.
44 M. J. Legorburu, R. M. Alonso, R. M. Jimenez and E. Ortiz, *J. Chromatogr. Sci.*, 1999, **37**, 283–287.
45 P. Pietta, A. Calatroni and A. Rava, *J. Chromatogr*., 1982, **12**, 377-381.
46 X. Gao, J. Chen, N. Mei, W. Tao, W. Jiang and X. Jiang, *Chromatographia*, 2005, **61**, 581–585.

47 F. Albu, C. Georgit, V. David and A. Medvedovici, *J. Chromatogr., B: Anal. Technol. Biomed. Life Sc*i., 2005, 816, 35-40.
48 D. Zendelovska, T. Stafilov and M. Stefova, *J. Chromatogr., B:Anal. Technol. Biomed. Life Sci*., 2003, **788**, 199–206.